OXFORD

Human Molecular Genetics, 2024, Vol. 33, R1, R34–R41
https://doi.org/10.1093/hmg/ddae036
Review Article

Central dogma rates in human mitochondria

Erik McShane and L. Stirling Churchman*

Department of Genetics, Blavatnik Institute, Harvard Medical School, 25 Shattuck Street, Boston, MA 02115, United States

*Corresponding author. Department of Genetics, Blavatnik Institute, 25 Shattuck Street, Harvard Medical School, Boston, MA 02115, United States.
E-mail: churchman@genetics.med.harvard.edu

Abstract

In human cells, the nuclear and mitochondrial genomes engage in a complex interplay to produce dual-encoded oxidative phosphorylation (OXPHOS) complexes. The coordination of these dynamic gene expression processes is essential for producing matched amounts of OXPHOS protein subunits. This review focuses on our current understanding of the mitochondrial central dogma rates, highlighting the striking differences in gene expression rates between mitochondrial and nuclear genes. We synthesize a coherent model of mitochondrial gene expression kinetics, highlighting the emerging principles and emphasizing where more precise measurements would be beneficial. Such an understanding is pivotal for grasping the unique aspects of mitochondrial function and its role in cellular energetics, and it has profound implications for aging, metabolic disorders, and neurodegenerative diseases.

Keywords: mitochondrial DNA; mitonuclear balance; oxidative phosphorylation; gene regulation

Introduction

The central dogma of molecular biology, first proposed by Francis Crick, describes the unidirectional flow of information from DNA to RNA to protein. This process takes on a unique character in mitochondria due to their distinct genome and specialized transcription and translation machinery (Fig. 1A) [1, 2]. Traditionally, mitochondrial research has emphasized a static view of gene expression, focusing on the molecular mechanisms and steady-state profiles of the proteome and transcriptome. However, understanding the dynamic aspects of this process is essential, particularly in the biogenesis of dual-encoded oxidative phosphorylation (OXPHOS) complexes. The coordination between nuclear and mitochondrial genomes in producing the correct quantities of OXPHOS subunits represents a pinnacle of cellular gene expression complexity [3].

OXPHOS complexes are composed of a precise assembly of subunits, with most subunits present in a singular copy. Achieving and controlling the steady-state levels of these protein subunits involves processes with measurable kinetics, such as mRNA transcription and protein degradation. Crucially, the same quantity of protein subunits can be achieved through nearly limitless permutations of these gene expression rates [4]. For instance, the production of an equivalent number of proteins can be achieved by either 10 mRNAs being translated at a rate of 1 protein per minute or a single mRNA being translated at 10 proteins per minute. Determining these kinetics is key not only to comprehending how cells function under healthy conditions but also in scenarios where imbalances in synthesis from the nuclear and mitochondrial genomes result in aging phenotypes, metabolic disorders, or neurodegenerative diseases [5–8]. Furthermore, the importance of understanding gene expression kinetics is underscored by the fact that many genes involved in mitochondrial gene expression, and therefore in setting the rates, are linked to human diseases [5].

Recent advancements in next-generation sequencing and proteomics have greatly enhanced our understanding of these dynamic processes in human mitochondria, offering new insights into the gene expression kinetics between mitochondrial and nuclear-encoded genes. This review aims to integrate these data, forming a coherent model of mitochondrial gene expression kinetics and identifying areas requiring more direct or refined measurements. Such understanding is vital for grasping the unique aspects of mitochondrial function and its critical role in cellular energetics.

Transcription rates

Production rate

Mitochondrial-encoded mRNAs (mt-mRNA) are the most abundant mRNA in the human cell and up to 30% of mRNA in energy-demanding tissues like muscle consists of mt-mRNA [9]. Accordingly, the transcriptional output from mitochondrial DNA (mtDNA) must be very high. We recently measured RNA turnover and abundance using TimeLapse-sequencing [10] and found that, in HeLa cells, mt-mRNA production was on average 1100-fold higher than for nuclear-encoded OXPHOS subunit mRNA (Fig. 2B) [11]. What does this mean in absolute numbers? Assuming 5 nuclear-encoded OXPHOS mRNA/hour in HeLa cells [4, 12] gives a production rate of about 5500 mt-mRNA per hour. Alternatively, the transcription rate of mtDNA can be computed from the absolute abundances and half-lives of mt-mRNA molecules as reported in [13] (Box 1). This calculation yields a median production rate of 9200 (+/− 4700) mt-mRNA/hour. Furthermore, in 1969, Giuseppe and Barbara Attardi estimated the overall mitochondrial transcription output in HeLa cells to be 4 million nucleotides per cell and minute [14]. This translates to about 16 000 primary transcripts (average 15 kb long) per hour and cell. Assuming similar synthesis from both the light and heavy strands

Received: December 28, 2023. **Revised:** December 28, 2023. **Accepted:** February 29, 2024

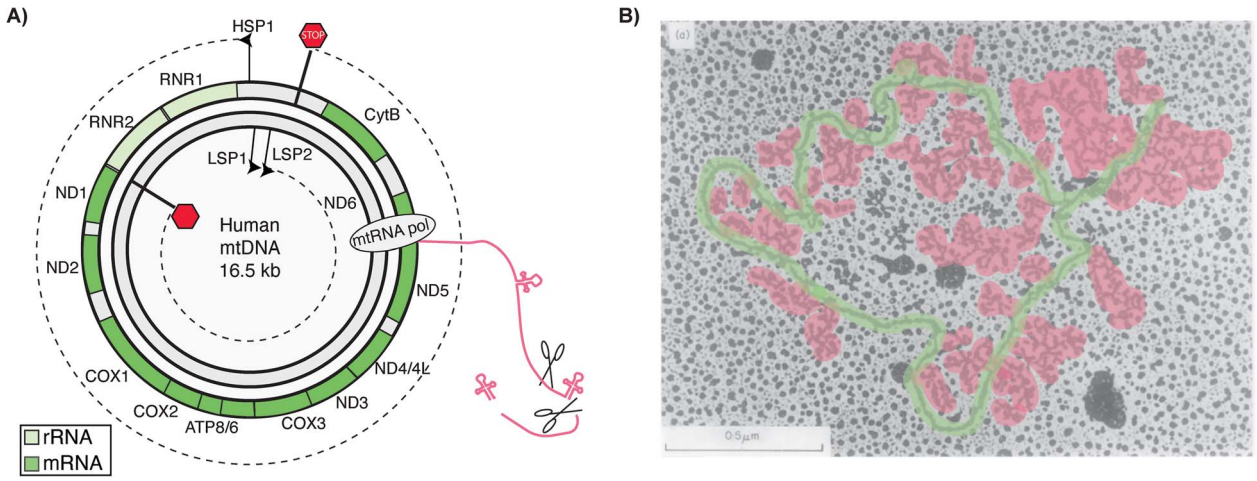

Figure 1. Primer on mitochondrial transcription. (A) The circular and highly polyploid mitochondrial genome (mtDNA) encodes two mitoribosomal rRNA, a full set of tRNA, and 13 proteins on 11 mRNA (two are bicistronic). The mtDNA is transcribed from three promoters, one on the heavy strand (HSP) and two on the light strand (LSP1 and 2) [67], located upstream of most genes. Transcription initiation requires the two transcription factors TFAM and TFBM2 as well as the single subunit RNA polymerase (POLRMT) which then associates with the transcription elongation factor (TEFM) [18]. Virtually, the entire 16.5 kb of mtDNA is transcribed into primary transcripts, and termination occurs before the antisense rRNA on the light strand and in the regulatory region on the heavy strand. The primary transcript is then cleaved into individual mRNA, tRNA, and rRNA. (B) An electron microscopy image of mtDNA (green color, added here) actively engaged by POLRMT with RNA (red color, added here) protruding [26]. The authors note that "At least 25 [RNA] bushes of various sizes can be seen attached to the circular DNA." and that "No clear pattern of size change of the bushes along the mtDNA molecule can be observed".

of mtDNA [11, 13, 15], the estimated transcription rate is around 8000 mt-mRNA produced per hour.

Box 1. Kinetics in Gene Expression: Understanding the Main Rates

Within biological systems we can use differential equations to model the abundance of their molecules and how this abundance changes over time. In the simplest terms, we can describe the change of abundance over time as the rate of molecules produced minus the rate of molecules removed:

$$\textbf{Change in abundance over time} = \textbf{Production rate} - [\textbf{Degradation rate}^{*}\ \textbf{Abundance}]$$

Change in abundance over time: represents the change in molecule abundance over time with the units of molecules/time.
Production rate: represents the synthesis rate of the molecule, with units of molecules/time.
Abundance: has the units of molecules.
Degradation rate: marks the pace at which molecules are broken down in cells, customarily indicated in 1/time.

This model allows us to represent our kinetic rates of interest (Production and Degradation rates). To obtain these rates we can fit the model to experimental data that captures the change of molecule abundance as a function of time.

Many biological systems exist in steady states. A steady state is defined as a zero net change in abundance over time, implying that the amount of molecules being added to the system is equivalent to the amount of molecules leaving the system. This can be represented by setting the change in abundance over time = 0 which gives us the following derivations:

$$\textbf{Change in abundance over time} = 0 = \textbf{Production rate} - [\textbf{Degradation rate}^{*}\ \textbf{Abundance}]$$

$$\textbf{Production rate} = \textbf{Degradation rate}^{*}\ \textbf{Abundance}$$

We can now try out this formula using numbers from Chujo *et al* [13]. They find that the steady-state abundance of COX1 is 37 000 mRNA/cell and the mRNA half-life is 166 min (= 2.8 h) which gives a degradation rate of 0.25/h. From these values, we can calculate a production rate of 9300 COX1 mRNA/h. This will be a good approximation, as mt-mRNA are very unstable, of how many molecules are synthesized but when the biomolecule is stable relative to the cell doubling time we need to take into account the fact that the cells grow and divide over time (for an example see [12]).

Note that, as above, degradation rates are commonly expressed in terms of half-lives, the time required for a particular molecular quantity to decrease by half. We can easily convert between the two using the following formula:

$$\text{Half} - \text{life} = \ln(2)/\text{Degradation rate}$$

These astounding numbers can be verified using orthogonal strategies. Mass spectrometric quantification of mitoribosome subunits found about 300 000 mitoribosomes per HeLa cell [16, 17]. Assuming that the subunit numbers reflect actual numbers of mitoribosomes, which need to double each cell cycle, proliferating cells must produce about 300 000 mitoribosomes every 26 h [11], or 11 500 mt-rRNA per hour. Given the polycistronic nature of mitochondrial transcription, the mt-rRNA production is expected to largely reflect heavy-strand encoded mRNA production [11, 18]. Using different methods and data we converge on a value on the order of 8500 copies (range 5500–11 500) of each mRNA and

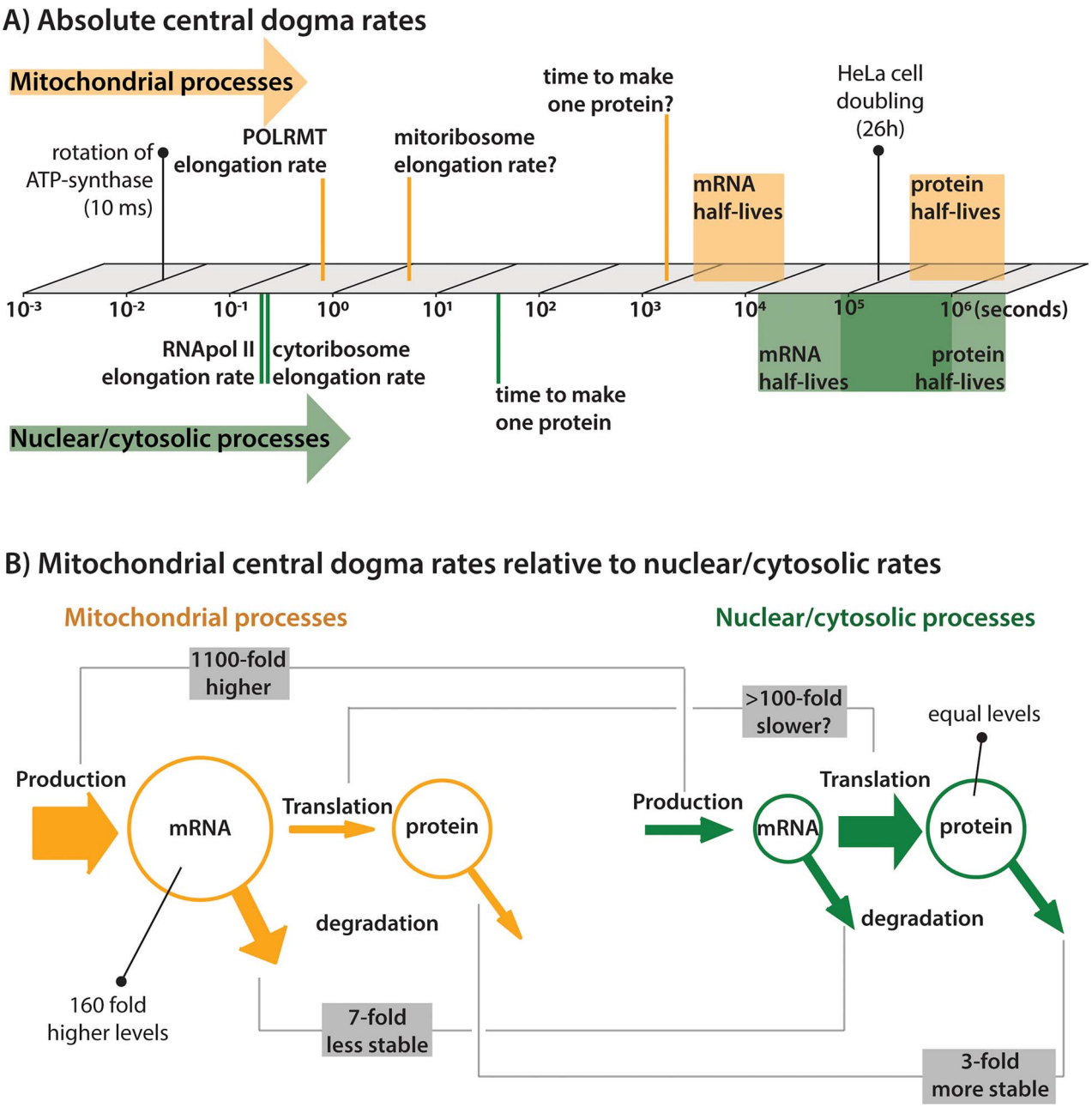

Figure 2. Absolute and relative central dogma rates. (A) Summary of absolute rates discussed in the main text. All elongation rates are in seconds/codon. The time to make one protein was calculated as follows: average coding sequence/translation elongation rate. (B) Summary of the mitochondrial rates relative to nuclear-encoded OXPHOS genes, discussed in the text. The figure was inspired by [68].

noncoding RNA per hour and cell (i.e. 93 500 total copies of the 11 mt-mRNA/hour).

Transcription initiation rate

High levels of mitochondrial transcription are partially enabled by the highly polyploid nature of mtDNA, although most copies are transcriptionally inactive at any one time. For example, only 11.7% of nucleoids in human fibroblast are specifically transcriptionally active (in contrast to being both transcriptionally and replicative active) [19]. These numbers are consistent with mtDNA accessibility measurements in HeLa cells [20]. Assuming 12% transcriptionally active mtDNA molecules out of 1000 total cellular nucleoids (estimates range broadly in HeLa cells 700–1000 [21], 7200 [22], 8800 [23] mtDNA copies per cell) and 17 000 primary transcripts (8500 from each strand) results in about 142 initiations per hour and mtDNA molecule or 25 s between initiation events.

Transcription elongation rate

Transcription elongation by the human mitochondrial RNA polymerase (POLRMT) is thought to be considerably slower than for other single unit RNA polymerases like the T7 RNAP (10 times faster than POLRMT) or the yeast mitochondrial RNA polymerase, Rpo1 (5 times faster) [24]. *In vitro* measurements of mitochondrial transcription elongation rates range between 0.22 to 0.72 kb/min. This rate is also considerably slower than nuclear RNA pol II elongation (> 2 kb/min) [25]. If these very slow elongation rates hold up *in vivo*, it leads to some interesting consequences. The average length of the light and heavy strand primary transcripts

is 15 kb; assuming an elongation rate of 0.5 kb/min, a full transcription cycle would take 30 min. Given an initiation event every 25 s, we would expect ~70 actively transcribing POLRMT per mtDNA, which is higher than the 25 POLRMT per molecule measured by electron microscopy of HeLa mtDNA molecules (Fig. 1B) [26]. This discrepancy could mean that the measurement should be revisited or one or more of our assumptions need to be adjusted. For example, if the elongation rate of POLRMT is twice as fast *in vivo*, and instead of just 12%, 17% of mtDNA molecules are transcriptionally active, then we would expect 25 POLRMTs per mtDNA. In either case, 70 actively transcribing POLRMT on 120 mtDNA molecules would result in 8400 active POLRMT per cell, a small fraction of the > 100 000 POLRMT molecules in a human cell [16, 17]. Many of these molecules are likely in an inactive state induced by dimerization via the non-coding RNA (7S RNA) [27]. Furthermore, this flurry of transcriptional activity might contribute to the robust occurrence of mitochondrial RNA granules [28, 29], especially considering how quickly mRNA is likely to pass through the granule (see "processing kinetics" below). Another aspect worth considering is that crowding on a mtDNA molecule might result in frequent head-on collisions of POLRMT transcribing opposing strands. If some collisions result in transcription termination we would expect decreased levels of promotor-distal-encoded RNA, something that has been described for nuclear-encoded genes in yeast [30]. Interestingly, promotor distal transcripts are less abundant than expected from turnover alone [11]. Furthermore, increasing transcription initiation rates, by depletion of the negative transcriptional regulator MTERF3 in mice, further decreases the levels of distally encoded transcripts [31].

RNA processing rates

RNA cleavage out of the primary transcript

The majority of mt-mRNA are flanked by tRNA and are cleaved out by tRNA processing enzymes [32]. At least in mice, 5′ tRNA processing of the tRNA (i.e. 3′ of any flanking mRNA) by RNAse P precedes 3′ tRNA processing by the RNAse Z [33, 34]. A few mRNAs lack a 3′ or 5′ flanking tRNA, and these noncanonical processing sites are processed by other enzymes such as members of the FASTK protein family [35]. We recently estimated RNA processing rates and found them to be very rapid in human mitochondria [11]. Most mt-mRNA are processed within a minute of transcription. However, the tricistronic *ATP6/8-COX3* mRNA, $tRNA^{Leu1}$*-ND1*, and *antisense-tRNA-COX1* all take tens of minutes to be processed. Nevertheless, considering the slow transcription elongation rates, discussed above, the predominantly quick processing rates indicate that processing is a co-transcriptional process. This is consistent with the fact that TEFM, the mitochondrial transcription elongation factor, is associated with RNA cleavage enzymes and that RNA processing is impaired in the absence of TEFM [36]. It is also consistent with electron microscopy showing no correlation between location on mtDNA and RNA length as would be expected if processing is post-transcriptional [26].

Polyadenylation rates of mt-mRNA

mt-mRNA (except *ND6*) are polyadenylated by the mitochondrial poly(A) polymerase but bear much shorter (40–60 nt) poly(A) tails than nuclear-encoded transcripts [37, 38]. For most transcripts, the poly(A) tail is required to complete the stop codon. Polyadenylation occurs rapidly following 3′-end cleavage even on transcripts that are yet to be processed on the 5′-end [11]. Poly(A) tails on 5′-end unprocessed mRNA were somewhat shorter than poly(A) tails on mature transcripts. The fact that a difference in poly(A) tail length is observable indicates that although initiation is a rapid process, poly(A) extension might still require some time for completion.

RNA turnover rates

Although mt-mRNA production is 1100-fold higher than for nuclear-encoded OXPHOS genes, mt-mRNA "only" accumulates to 160-fold higher levels [11]. The lower level of mt-mRNA at steady state is due to mt-mRNA being rapidly turned over. On average mt-mRNA is degraded 7-fold faster than nuclear-encoded OXPHOS mRNA [11]. The high mt-mRNA turnover rates are most likely a result of the coupling between noncoding and coding RNA production in mitochondria (Box 2), as rapid degradation is needed to prevent mt-mRNA from accumulating to the same levels as the rRNA and tRNA. For example, if mt-mRNA had the same slow turnover rate as mt-rRNA, they would represent 70% of the HeLa cellular mRNA pool instead of the 6% it does actually [11].

Box 2. What sets transcription rates in mitochondria?

The polycistronic nature of mitochondrial transcription requires that either mRNA, rRNA, or tRNA production drives overall transcription rates to ensure adequate production of the RNA required in the largest amounts. We found that the production rate of mt-mRNA is set to similar level as mt-rRNA, which are likely one of the most abundant transcripts in mitochondria [11]. Although mt-tRNAs are also plentiful, tRNA levels are usually substoichiometric to rRNA in human cytosolic ribosomes and *E. coli* [65], suggesting that rRNA sets the overall transcriptional output in mitochondria. However, $tRNA^{val}$, which is encoded between the two rRNA genes, may be the limiting factor in transcription, as it acts both as a tRNA and as a structural component of the mitoribosome, where it replaces the 5S RNA found in bacterial and human ribosomes [66].

The degradation of mt-RNA is a critical process that goes beyond simply setting the overall levels of transcripts. Because mitochondrial transcription is polycistronic, with transcripts encoded on the same strand being produced at nearly equal rates [11], RNA degradation has been proposed to dictate the relative levels of mitochondrial transcripts [13, 18, 39]. Our careful measurements of the production and turnover rates of mt-mRNA showed that RNA turnover alone could explain more than 86% of the variability in mitochondrial mRNA levels. Furthermore, this connection between RNA turnover and relative transcript abundance holds even in cells lacking the key RNA-stabilizing protein, leucine-rich pentatricopeptide repeat containing (LRPPRC) [11, 13].

Translation rates

Mitochondrial translation is performed by specialized protein-rich mitochondrial ribosomes (mitoribosomes). The mitoribosomes are membrane-bound and translate the mitochondrial-encoded OXPHOS subunits directly into the inner mitochondrial membrane [40]. The first step in translation initiation is mRNA binding either a mitoribosomal monosome or small subunit [41]. Mitochondrial mRNA associates rapidly with mitoribosomes, with rates ranging from 4 to 13 min with a median of 5 min [11]. This is much faster than for nuclear-encoded OXPHOS mRNA, which

take 176 min on average to reach cytoribosomes, even 6 min after nuclear export [11, 42]. This long delay is in accordance with the more complex processing and transport processes of nuclear-encoded mRNA.

Due to the high number of mt-mRNAs and faster ribosome association relative to the nuclear-encoded OXPHOS mRNA, many more mt-mRNAs are expected to be bound by mitoribosomes than nuclear-encoded mRNAs translated by cytosolic ribosomes. Given this, we postulated that mitochondrial translation rates must be more than 100-fold slower than cytosolic translation rates to balance protein production between the two compartments [11]. The lack of assays to measure mitochondrial translation rates made this hypothesis difficult to test. However, a recent report identified the antibiotic retapamulin as a mitoribosome translation initiation inhibitor [43]. By using retapamulin in ribosome run-off assays, the authors were able to measure elongation rates of 0.42 codons per second (or 1.26 nt/s). Combining this information with estimations of the number of mitoribosomes occupying an individual mt-mRNA (on average 2 mitoribosomes/mt-mRNA, spaced 672 nt apart) the authors estimated translation initiation rates at 533 s/initiation [43]. Furthermore, the authors measured mt-mRNA turnover rates and calculated lifetime translation rates of 26 rounds of translation per mRNA (99 min average lifetime) giving an overall translation rate of about 15 proteins/mRNA*hour. These numbers, match our expectations [11] and are much slower than estimates for cytosolic translation which ranges between 1 and 20 s/initiation and 180 to 3600 proteins/mRNA*h [4, 44].

Production rates for the OXPHOS subunits vary extensively

On average OXPHOS complex subunits are expected to be synthesized in matched amounts between the nuclear- and mitochondrial-encoded genes [8]. However, detailed analyses of relative protein synthesis rates of nuclear-encoded [8, 45] and mitochondrial-encoded OXPHOS subunits [8] have revealed large differences in the synthesis rates of subunits that are expected to exist in a 1 to 1 ratio in the final OXPHOS complex. For example, Complex I subunits are produced in starkly non-stoichiometric amounts (Fig. 3A). This discrepancy is expected to be resolved primarily at the level of protein degradation (Fig. 3B).

Protein degradation rates

Protein degradation is a highly regulated multifunctional process executed by a distinct set of mitochondrial proteases [46, 47]. Recently, stable isotope labeling by amino acids (SILAC) in combination with mass spectrometric analysis has become a favorite tool to measure protein synthesis and turnover in mitochondria. For example, in a study of the human mitochondrial high-confidence proteome (MitoCoP) [16] the turnover kinetics of the majority of the mitochondrial proteome was quantified. In HeLa cells, protein half-lives range from 1.6 h to weeks. Interestingly, half-lives of OXPHOS complexes and the mitoribosome subunits ranged considerably even within the same complex. For example, the half-lives of Complex I subunits range from 11 h to > 370 h (Fig. 3C). The average half-life of Complex I subunits located in the matrix arm (25 h) is less than half that of the average half-life of the membrane-incorporated subunits (58 h), which could relate to the greater damage from reactive oxygen species to the matrix-facing subunits. Interestingly, the mitochondrial-encoded subunits are consistently among the most stable subunits in each OXPHOS complex (e.g. the median half-life of mitochondrially encoded subunits in Complex I is 185 h compared to 47 h for nuclear-encoded subunits). Overall, the large range of subunit stabilities might explain the need for the dispersed protein synthesis rates discussed above [45]. However, as degradation rates far surpass cell doubling times, production rates are expected to be set mainly by the need to double cellular biomass each cell doubling rather than replacing subunits lost to degradation, at least in proliferating cell culture systems.

Another interesting aspect is the degradation of excess unassembled (orphaned) subunits which is a common phenomenon in human cells [48, 49] (Fig. 3B). Many subunits of OXPHOS and mitoribosome complexes require assembly for their stability [50–52]. For example, nuclear-encoded mitoribosome and OXPHOS subunits are made in excess and degraded during assembly in HeLa cells [53, 54]. Furthermore, there is probably a significant amount of co-translation protein quality control occurring in human cells [55] as in yeast [56]. Finally, the fine-tuning of protein production by protein degradation could provide significant benefits for the minimal mitochondrial gene expression system, rendering it more robust to gene expression variability and noise with a decreased dependence on precisely coordinated protein synthesis [48].

Discussion and outlook: Gene expression control *in vivo*

By delineating the rates of each gene expression step, we can start untangling at what stages gene expression control is exerted. For example, transcription rates are largely responsible for and thus predict the nuclear-encoded OXPHOS transcriptome, while RNA degradation explains the mitochondrial transcriptome [11]. Thus we would expect that mRNA level control in mitochondria would be mainly exerted via proteins involved in RNA turnover such as LRPPRC [57], while transcription factors would be more important for the regulation of nuclear-encoded genes. Importantly, the kinetics of steps such as subunit import into mitochondria [58] and protein complex assembly, which are not strictly speaking central dogma rates and not discussed here, are also crucially important for understanding mitochondrial gene expression. For example, the complete assembly of the mitoribosome was estimated to take 2–3 h in HeLa cells [54], longer than the production rates of the individual rRNA, tRNA, and protein subunits.

Where will the field go? A caveat associated with most of the results discussed here is the predominance of cell culture work in immortalized or cancer cell lines. Nevertheless, it's important to note that most of the findings in human cells hold up in animal models and vice versa. An increased focus on and development of dynamic measurements in model organisms such as the fly [59] or mouse [60] will continue to be invaluable for our understanding. Another issue is that most work discussed here averages over millions of cells. Interestingly, recent single-cell analyses have been valuable for understanding mitochondrial gene expression kinetics [61, 62] and the advent of single-cell proteomics will open up new avenues of research [63]. Furthermore, the discovery of specialization of populations of mitochondria [64] and the fact that mitochondria can be highly heteroplasmic will require subcellular resolution in kinetic measurements. Ultimately, advancing our understanding of the interplay between nuclear and mitochondrial gene expression processes necessitates a multidisciplinary approach, integrating findings from cell culture, animal models, and emerging single-cell technologies to fully decipher the molecular underpinnings of mitochondrial diseases and their broader biological significance.

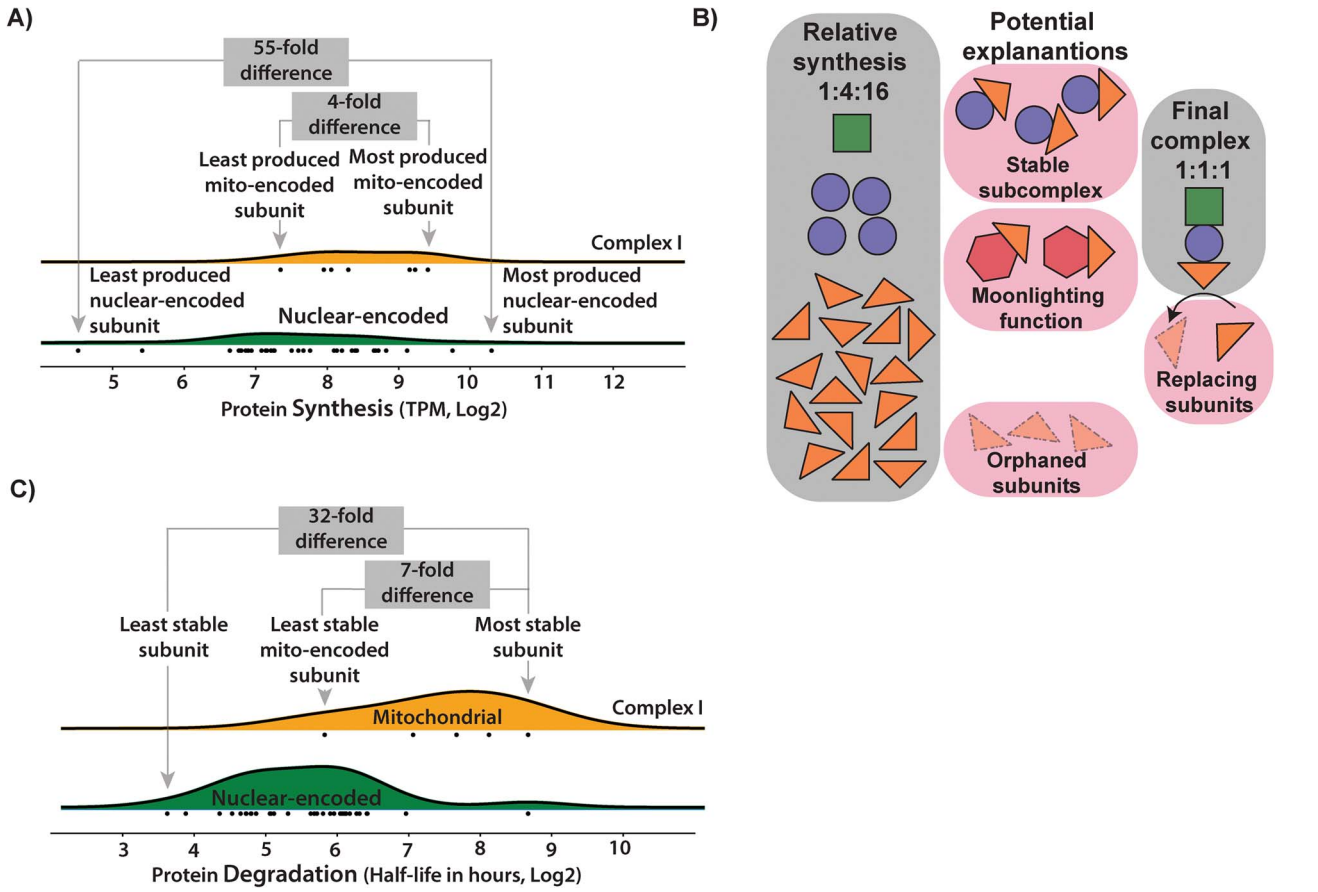

Figure 3. Protein synthesis and degradation are non-stoichiometric. (A) Protein synthesis, as judged by mito- and cytoribosome profiling, does not show equimolar production of subunits that are expected to exist in the same amounts in the assembled complex (data from [8]). Shown here are complex I subunits in HeLa cells but other OXPHOS complexes display a similar spread in synthesis rates and the results are reproducible in other cell lines [8]. Note that the synthesis levels are not directly comparable between nuclear and mitochondrially encoded subunits as they are from different experiments. (B) Non-stoichiometric subunit production can be explained by multiple not mutually-exclusive mechanisms. In this example, one subunit is synthesized in 16-fold excess and another in 4-fold excess. This excess may be due to additional functions of these subunits or their accumulation in stable subcomplexes, necessitating higher production. Additionally, the varying stability of subunits before forming a complex and the need for replacing subunits in an already assembled complex also justify their increased synthesis rates. (C) Degradation rates range broadly for both nuclear and mitochondrially encoded subunits (data from [16]) although they are generally longer than cell doubling time (log2(26 h) = 4.7). Shown here are complex I subunits in HeLa cells but other OXPHOS complexes display a similar spread in turnover rates and the results are reproducible in other cell lines [16]. Note that the synthesis levels are directly comparable between nuclear and mitochondrially encoded subunits as they are from the same experiments. Half-lives determined to be infinite were here set to 370 h.

Acknowledgements

We would like to thank A. Raicu, M. Couvillion, and S. Isaac for their careful review of the manuscript, and A. Baxter-Koenigs for feedback on Box 1.

Conflict of interest statement: None declared.

Funding

This work was supported by National Institutes of Health grant R01-GM123002 (L.S.C.). E.M. is supported by European Molecular Biology Organization Long-Term Fellowship (ALTF 143-2018).

References

1. Rackham O, Filipovska A. Organization and expression of the mammalian mitochondrial genome. *Nat Rev Genet* 2022;**23**:606–23.
2. Tan BG, Gustafsson CM, Falkenberg M. Mechanisms and regulation of human mitochondrial transcription. *Nat Rev Mol Cell Biol* 2023;**25**:119–32.
3. Isaac RS, McShane E, Churchman LS. The multiple levels of Mitonuclear Coregulation. *Annu Rev Genet* 2018;**52**:511–33.
4. Hausser J, Mayo A, Keren L. *et al.* Central dogma rates and the trade-off between precision and economy in gene expression. *Nat Commun* 2019;**10**:68.
5. Suomalainen A, Battersby BJ. Mitochondrial diseases: the contribution of organelle stress responses to pathology. *Nat Rev Mol Cell Biol* 2017;**19**:77–92.
6. Kujoth GC, Hiona A, Pugh TD. *et al.* Mitochondrial DNA mutations, oxidative stress, and apoptosis in mammalian aging. *Science* 2005;**309**:481–4.
7. Song J, Herrmann JM, Becker T. Quality control of the mitochondrial proteome. *Nat Rev Mol Cell Biol* 2021;**22**:54–70.
8. Soto I, Couvillion M, Hansen KG. *et al.* Balanced mitochondrial and cytosolic translatomes underlie the biogenesis of human respiratory complexes. *Genome Biol* 2022;**23**:170.
9. Mercer TR, Neph S, Dinger ME. *et al.* The human mitochondrial transcriptome. *Cell* 2011;**146**:645–58.
10. Schofield JA, Duffy EE, Kiefer L. *et al.* TimeLapse-seq: adding a temporal dimension to RNA sequencing through nucleoside recoding. *Nat Methods* 2018;**15**:221–5.

11. McShane E, Couvillion M, Ietswaart R. *et al.* A kinetic dichotomy between mitochondrial and nuclear gene expression drives OXPHOS biogenesis. *Mol Cell* 2024. https://doi.org/10.1016/j.molcel.2024.02.028.
12. Schwanhäusser B, Busse D, Li N. *et al.* Global quantification of mammalian gene expression control. *Nature* 2011;**473**:337–42.
13. Chujo T, Ohira T, Sakaguchi Y. *et al.* LRPPRC/SLIRP suppresses PNPase-mediated mRNA decay and promotes polyadenylation in human mitochondria. *Nucleic Acids Res* 2012;**40**:8033–47.
14. Attardi G, Attardi B. The informational role of mitochondrial DNA. In: Hanley E.W. (ed.), *Problems in biology: RNA in development*. Salt Lake City: University of Utah Press, 1970, 245–83.
15. Aloni Y, Attardi G. Symmetrical in vivo transcription of mitochondrial DNA in HeLa cells. *Proc Natl Acad Sci USA* 1971;**68**:1757–61.
16. Morgenstern M, Peikert CD, Lübbert P. *et al.* Quantitative high-confidence human mitochondrial proteome and its dynamics in cellular context. *Cell Metab* 2021;**33**:2464–2483.e18.
17. Bekker-Jensen DB, Kelstrup CD, Batth TS. *et al.* An optimized shotgun strategy for the rapid generation of comprehensive human proteomes. *Cell Syst* 2017;**4**:587–599.e4.
18. Miranda M, Bonekamp NA, Kühl I. Starting the engine of the powerhouse: mitochondrial transcription and beyond. *Biol Chem* 2022;**403**:779–805.
19. Brüser C, Keller-Findeisen J, Jakobs S. The TFAM-to-mtDNA ratio defines inner-cellular nucleoid populations with distinct activity levels. *Cell Rep* 2021;**37**:110000.
20. Stefan Isaac R, Tullius TW, Hansen KG. *et al.* Single-nucleoid architecture reveals heterogeneous packaging of mitochondrial DNA. Single-nucleoid architecture reveals heterogeneous packaging of mitochondrial DNA. *Nat Struct Mol Biol* 2024. https://doi.org/10.1038/s41594-024-01225-6.
21. Kozhukhar N, Fant A, Alexeyev MF. Quantification of mtDNA content in cultured cells by direct droplet digital PCR. *Mitochondrion* 2021;**61**:102–13.
22. Shmookler Reis RJ, Goldstein S. Mitochondrial DNA in mortal and immortal human cells. Genome number, integrity, and methylation. *J Biol Chem* 1983;**258**:9078–85.
23. Bogenhagen D, Clayton DA. The number of mitochondrial deoxyribonucleic acid genomes in mouse L and human HeLa cells. Quantitative isolation of mitochondrial deoxyribonucleic acid. *J Biol Chem* 1974;**249**:7991–5.
24. Sultana S, Solotchi M, Ramachandran A. *et al.* Transcriptional fidelities of human mitochondrial POLRMT, yeast mitochondrial Rpo41, and phage T7 single-subunit RNA polymerases. *J Biol Chem* 2017;**292**:18145–60.
25. Fuchs G, Voichek Y, Benjamin S. *et al.* 4sUDRB-seq: measuring genomewide transcriptional elongation rates and initiation frequencies within cells. *Genome Biol* 2014;**15**:R69.
26. Aloni Y, Attardi G. Expression of the mitochondrial genome in HeLa cells. XI. Isolation and characterization of transcription complexes of mitochondrial DNA. *J Mol Biol* 1972;**70**:363–73.
27. Zhu X, Xie X, Das H. *et al.* Non-coding 7S RNA inhibits transcription via mitochondrial RNA polymerase dimerization. *Cell* 2022;**185**:2309–2323.e24.
28. Jourdain AA, Koppen M, Wydro M. *et al.* GRSF1 regulates RNA processing in mitochondrial RNA granules. *Cell Metab* 2013;**17**:399–410.
29. Antonicka H, Sasarman F, Nishimura T. *et al.* The mitochondrial RNA-binding protein GRSF1 localizes to RNA granules and is required for posttranscriptional mitochondrial gene expression. *Cell Metab* 2013;**17**:386–98.
30. Prescott EM, Proudfoot NJ. Transcriptional collision between convergent genes in budding yeast. *Proc Natl Acad Sci* 2002;**99**:8796–801.
31. Park CB, Asin-Cayuela J, Cámara Y. *et al.* MTERF3 is a negative regulator of mammalian mtDNA transcription. *Cell* 2007;**130**:273–85.
32. Ojala D, Merkel C, Gelfand R. *et al.* The tRNA genes punctuate the reading of genetic information in human mitochondrial DNA. *Cell* 1980;**22**:393–403.
33. Rackham O, Busch JD, Matic S. *et al.* Hierarchical RNA processing is required for mitochondrial ribosome assembly. *Cell Rep* 2016;**16**:1874–90.
34. Kuznetsova I, Siira SJ, Shearwood A-MJ. *et al.* Simultaneous processing and degradation of mitochondrial RNAs revealed by circularized RNA sequencing. *Nucleic Acids Res* 2017;**45**:5487–500.
35. Ohkubo A, Van Haute L, Rudler DL. *et al.* The FASTK family proteins fine-tune mitochondrial RNA processing. *PLoS Genet* 2021;**17**:e1009873.
36. Jiang S, Koolmeister C, Misic J. *et al.* TEFM regulates both transcription elongation and RNA processing in mitochondria. *EMBO Rep* 2019;**20**:e48101.
37. Rackham O, Mercer TR, Filipovska A. The human mitochondrial transcriptome and the RNA-binding proteins that regulate its expression. *Wiley Interdiscip Rev RNA* 2012;**3**:675–95.
38. Bratic A, Clemente P, Calvo-Garrido J. *et al.* Mitochondrial polyadenylation is a one-step process required for mRNA integrity and tRNA maturation. *PLoS Genet* 2016;**12**:e1006028.
39. Piechota J, Tomecki R, Gewartowski K. *et al.* Differential stability of mitochondrial mRNA in HeLa cells. *Acta Biochim Pol* 2006;**53**:157–68.
40. Itoh Y, Andréll J, Choi A. *et al.* Mechanism of membrane-tethered mitochondrial protein synthesis. *Science* 2021;**371**:846–9.
41. Remes C, Khawaja A, Pearce SF. *et al.* Translation initiation of leaderless and polycistronic transcripts in mammalian mitochondria. *Nucleic Acids Res* 2023;**51**:891–907.
42. Smalec BM, Ietswaart R, Choquet K. *et al.* Genome-wide quantification of RNA flow across subcellular compartments reveals determinants of the mammalian transcript life cycle. Genome-wide quantification of RNA flow across subcellular compartments reveals determinants of the mammalian transcript life cycle. 2022; *bioRxiv* (2022) , 2022.08.21.504696.
43. Wakigawa T, Mito M, Yamashiro H. *et al.* Complexity and dynamics of in organello translation landscape assessed by high-resolution mitochondrial ribosome profiling. Complexity and dynamics of in organello translation landscape assessed by high-resolution mitochondrial ribosome profiling. 2023; *bioRxiv* (2023) , 2023.07.19.549812.
44. Morisaki T, Stasevich TJ. Quantifying single mRNA translation kinetics in living cells. *Cold Spring Harb Perspect Biol* 2018;**10**:a032078.
45. Taggart JC, Li G-W. Production of protein-complex components is stoichiometric and lacks general feedback regulation in eukaryotes. *Cell Syst* 2018;**7**:580–589.e4.
46. Deshwal S, Fiedler KU, Langer T. Mitochondrial proteases: multifaceted regulators of mitochondrial plasticity. *Annu Rev Biochem* 2020;**89**:501–28.
47. McShane E, Selbach M. Physiological functions of intracellular protein degradation. *Annu Rev Cell Dev Biol* 2022;**38**:241–62.
48. Taggart JC, Zauber H, Selbach M. *et al.* Keeping the proportions of protein complex components in check. *Cell Syst* 2020;**10**:125–32.

49. McShane E, Sin C, Zauber H. *et al.* Kinetic analysis of protein stability reveals age-dependent degradation. *Cell* 2016;**167**: 803–815.e21.
50. Imami K, Selbach M, Ishihama Y. Monitoring mitochondrial translation by pulse SILAC. *J Biol Chem* 2023;**299**:102865.
51. Stroud DA, Surgenor EE, Formosa LE. *et al.* Accessory subunits are integral for assembly and function of human mitochondrial complex I. *Nature* 2016;**538**:123–6.
52. Zurita Rendón O, Shoubridge EA. Early complex I assembly defects result in rapid turnover of the ND1 subunit. *Hum Mol Genet* 2012;**21**:3815–24.
53. Bogenhagen DF, Haley JD. Pulse-chase SILAC-based analyses reveal selective over-synthesis and rapid turnover of mitochondrial protein components of respiratory complexes. *J Biol Chem* 2020;**295**:2544–54.
54. Bogenhagen DF, Ostermeyer-Fay AG, Haley JD. *et al.* Kinetics and mechanism of mammalian mitochondrial ribosome assembly. *Cell Rep* 2018;**22**:1935–44.
55. Poerschke S, Oeljeklaus S, Cruz-Zaragoza LD. *et al.* Identification of TMEM126A as OXA1L-interacting protein reveals cotranslational quality control in mitochondria. *Mol Cell* 2024;**84**: 345–358.e5.
56. Kohler A, Carlström A, Nolte H. *et al.* Early fate decision for mitochondrially encoded proteins by a molecular triage. *Mol Cell* 2023;**83**:3470–3484.e8.
57. Sasarman F, Brunel-Guitton C, Antonicka H. *et al.* LRPPRC and SLIRP interact in a ribonucleoprotein complex that regulates posttranscriptional gene expression in mitochondria. *Mol Biol Cell* 2010;**21**:1315–23.
58. Schäfer JA, Bozkurt S, Michaelis JB. *et al.* Global mitochondrial protein import proteomics reveal distinct regulation by translation and translocation machinery. *Mol Cell* 2022;**82**: 435–446.e7.
59. Rosenberger FA, Atanassov I, Moore D. *et al.* Stable isotope Labeling of amino acids in flies (SILAF) reveals differential phosphorylation of mitochondrial proteins upon loss of OXPHOS subunits. *Mol Cell Proteomics* 2021;**20**:100065.
60. Sheean ME, McShane E, Cheret C. *et al.* Activation of MAPK overrides the termination of myelin growth and replaces Nrg1/ErbB3 signals during Schwann cell development and myelination. *Genes Dev* 2014;**28**:290–303.
61. Replogle JM, Saunders RA, Pogson AN. *et al.* Mapping information-rich genotype-phenotype landscapes with genome-scale perturb-seq. *Cell* 2022;**185**:2559–2575.e28.
62. Xu Z, Sziraki A, Lee J. *et al.* Dissecting key regulators of transcriptome kinetics through scalable single-cell RNA profiling of pooled CRISPR screens. *Nat Biotechnol* 2023. https://doi.org/10.1038/s41587-023-01948-9.
63. Rosenberger FA, Thielert M, Mann M. Making single-cell proteomics biologically relevant. *Nat Methods* 2023;**20**: 320–3.
64. Benador IY, Veliova M, Mahdaviani K. *et al.* Mitochondria bound to lipid droplets have unique bioenergetics, composition, and dynamics that support lipid droplet expansion. *Cell Metab* 2018; **27**:869–885.e6.
65. Dong H, Nilsson L, Kurland CG. Co-variation of tRNA abundance and codon usage in Escherichia coli at different growth rates. *J Mol Biol* 1996;**260**:649–63.
66. Rorbach J, Gao F, Powell CA. *et al.* Human mitochondrial ribosomes can switch their structural RNA composition. *Proc Natl Acad Sci USA* 2016;**113**:12198–201.
67. Tan BG, Mutti CD, Shi Y. *et al.* The human mitochondrial genome contains a second light strand promoter. *Mol Cell* 2022;**82**:3646–3660.e9.
68. Moran U, Phillips R, Milo R. SnapShot: key numbers in biology. *Cell* 2010;**141**:1262–1262.e1.